ORIGINAL PAPER

UROLOGICAL ONCOLOGY

Methodology and evaluation of the renal arterial system

Tomasz Drewniak[1], Maciej Rzepecki[1], Kajetan Juszczak[1,5], Zbigniew Moczulski[4], Katarzyna Reczyńska[2], Małgorzata Jakubowska[3]

[1]Department of Urology, Rydygier Memorial Hospital, Cracow, Poland
[2]Faculty of Electrical Engineering, Automatics, Computer Science and Biomedical Engineering, AGH University of Science and Technology, Cracow, Poland
[3]Faculty of Materials Science and Ceramics, AGH University of Science and Technology, Cracow, Poland
[4]Department of Radiology, Rydygier Memorial Hospital, Cracow, Poland
[5]Department of Pathophysiology, Medical College Jagiellonian University, Cracow, Poland

Article history
Submitted: Feb. 12, 2013
Accepted: March 6, 2013

Correspondence
Tomasz Drewniak
Department of Urology
Rydygier Memorial Hospital
1, Złotej Jesieni Street
31–826 Cracow, Poland
phone: +48 126 468 764
urologiarydygier@vp.pl

Introduction. The broad range of medical images and image processing technologies are applied in urology. The aim was to propose methodology to assess three–dimensional (3D) arrangement of renal arterial tree and to build a statistical model for analyzing the layout of arteries in the sections of the kidney.

Methods. The series of kidney CT slices are analyzed using image processing procedures and further the 3D model of arterial systems is converted to a graph tree which includes information about features of the renal arterial system.

Results. The selected endocast was transformed to the form of the 3D connected tubes, further to the tree data structure and next analyzed. The information about 3D coordinates of the nodes, also branch length and diameter were stored. Renal arterial system of the considered kidney possessed 181 branches with 14 bifurcation levels. The number of branches was highest at the 9th bifurcation level. The mean length of the arterial branch on each bifurcation level was constant (6 mm). The branch diameters rapidly decreased after each bifurcation. The number of terminal branches increases up to 9th level where there are 19 terminal branches. The mean length of terminal arteries was 7.17 mm while the mean radius 0.46 mm. A statistically significant correlation between parameters that described sub–trees was noticed. It was observed that the individual artery segments occupy a separate space in the kidney volume.

Conclusions. The methodology has the potential to assist in presurgical planning based on branching patterns of the renal arterial system and corresponding pathology.

Key Words: renal arterial system ‹› computed tomography ‹› tree–like structures ‹› descriptive statistics of the renal arterial tree ‹› partial nephrectomy

INTRODUCTION

The broad range of medical images and image processing technologies, representing the integration of computer technology in presurgical planning and surgical procedures are often applied in urology [1]. Such systems can be seen as a combination of several procedures and tools developed in order to overcome the drawbacks of invasive surgery and helps the surgeon's orientation inside the three dimensional (3D) anatomy during surgery.

Partial nephrectomy (PN) has gained more importance in the treatment of patients with small renal masses [2, 3, 4] and it can be performed for selected tumors with a maximum diameter of 7 cm [5–10]. Moreover, the benefits of PN are well established and include, above all, a decreased risk of long–term renal insufficiency and consequently a positive impact on the quality of life [11, 12, 13]. The knowledge about kidney arteries branching is very important for safe performance of varies urological procedures. An invasive arteriography allows obtaining precise

DOI: 10.5173/ceju.2013.02.art10

but two–dimensional image (and) angio–CT can follow the renal arteries only up to their second branches. There is lack of strategies which enable imaging of the whole renal arterial pathway in presurgical planning. Therefore we proposed the novel self–developed approach for analyzing and improving the understanding of anatomical relationships between kidney endocasts of intrarenal arteries. We developed a multi–step approach for characterizing the tree–like structure of the renal blood vessels.

Several structures in the human physiology follow a tree–shaped morphology. Examples of such structures are the blood–vessel system, the airway tree of a lung, bronchial tree, nerve tissues, a lymphatic system, and the retinal vascular network, for example [14–17]. It should be underlined that less attention has been paid to the essentially three–dimensional than two–dimensional structures. Based on computer models of arterial trees, simulation studies have been frequently used to gain a better understanding of both diagnostic and therapeutic aspects of blood flow. By applying the strategy proposed in this work it is possible to generate an optimized arterial tree model tree in three dimensions. Additionally, these computerized image analysis techniques can then be applied to compute the desired features of the arterial system that are usually associated with function or pathology, and can be used in presurgical planning.

METHODS

The work presents the methodology of renal arterial trees analysis that consists of the following steps. First, the human kidney endocast is prepared. Then, the endocast is processed (transformed) to a numeric form using high–resolution computed tomography. To perform this type of analysis, a pre–processing step is usually required: the arteries are traced and extracted from the image, using manual or automated procedures. Additionally, the series of intersections is analyzed using our self–developed image processing procedures in a Matlab environment to find the contours in the CT scans, which defined the boundary of each artery.

Certain preprocessing steps are necessary before the tree–like structures are available for analysis. First, the structure outline needs to be traced and segmented from the rest of the tissue or background in the image. Then, the tree–like structures are reconstructed by identifying points of branching. The contours of each artery were connected to create a pipe–like shape. The arterial network is modeled as a branching tree of nonintersecting, rigid cylindrical tubes. Starting at the main renal artery (root segment), the tree successively bifurcates down to the last level, where the model tree is truncated in the form of terminal segments. The geometry of the tree is characterized by the Cartesian coordinates of the endpoint of each segment together with its actual (outer) radius.

The three–dimensional model of arterial systems is converted for further analysis to a graph tree constituting typical and convenient data structure. Tree–like structures are physical structures that may be modeled using computer data named trees. In particular, we focus on structures modeled by directed rooted trees, defined as *directed acyclic graphs* in which there exists only one path between any two nodes [18]. Each node has one or no parents, while the node at the top of the tree that has no parents is identified as the root of the tree. When the nodes of the tree are assigned labels, then the tree is referred to as a *labeled rooted tree.* In this paper we consider tree–like structures that represent the renal arterial system. In the proposed tree each node may possess up to four successors or child nodes.

Finally, the full information about parameters of the renal arterial system is evaluated and preserved, i.e. diameters and lengths of individual branches and coordinates of the nodes. Further, a statistical analysis of the renal arterial tree was realized by a Matlab software specifically designed for three–dimensional quantitative evaluation of arterial pathways.

Our experimental results demonstrate the effectiveness of the proposed method in automatically characterizing tree–like structures in kidney images. These methods can potentially provide insight to the relationship between branching topology and function or pathology.

RESULTS

In the work we applied the elaborated methodology and tools in evaluation of the selected, typical renal arterial system. The created data structure in the tree form was studied using software tools of descriptive statistics. The analyses mainly relied on exploration of the branch lengths, diameters, and volume distributions throughout the tree, and its location in the space.

First the endocast was imaged using a high–resolution CT and processed by various specialized procedures to form the 3D connected tubes (Figure 1). Further such image was converted to the form of tree data structure (Figure 2), in which the information about coordinates (x, y and z) of the nodes and also branch lengths and diameters was stored. The volume of the convex hull circumscribed on the analyzed arterial tree was about 53.5 cm^3, while the

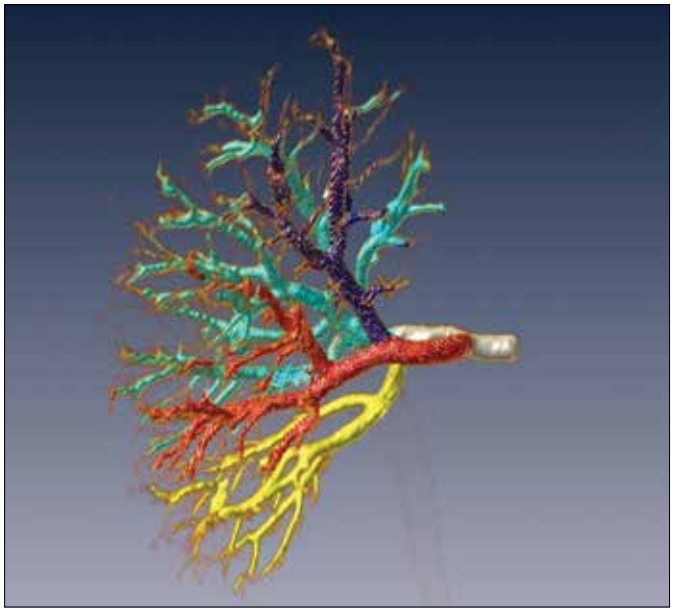

Figure 1. *Arterial system after high–resolution CT and image volume rendering processing (the subtrees were marked with different colours).*

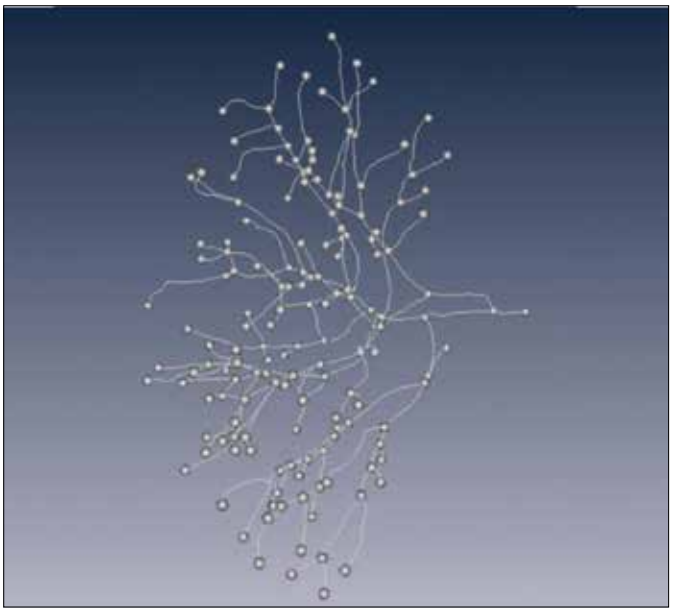

Figure 2. *Graph tree obtained from image presented in Figure 1. Black circles indicate nodes (bifurcation of the vessels).*

number of analyzed branches in the presented endocast was 181 with 14 bifurcation levels. The mean diameter of the artery in the tree root amounted to 4.58 mm, while the length – 6.03 mm. The number of branches was highest (n = 32) at the 9th bifurcation level (Figure 3). Figures 4 and 5 present, in the form of box–plot, the detailed descriptive statistic of the branch lengths and areas at respective bifurcation levels (the smallest observation, lower quartile, arithmetic mean, median, upper quartile, largest observation). It may be noticed that the mean length of the arterial branch on each bifurcation level was constant and amounted to approx. 6 mm. This conclusion did not regard the second or third level, in which the length was even 18 mm. The relevant dispersion of the branch length was observed. The branch diameters rapidly decreased after each bifurcation. The diameter of the main artery was approx. 4.58 mm and after the first division it was 4.26 mm and 3.60 mm. There was also noticed a relevant dispersion of the branched areas (RSD up to 80% at the 6^{th} and 7^{th} levels of the arterial tree).

It was observed (Figure 6) that the sum of areas of each level increased to the 6–7 bifurcation and further decreased (the number of branches of each level was lower). The reason of such situation may be explained by the decreasing blood pressure and flow speed. The highest sum of areas and volumes of the arteries was observed on the 6^{th} level (55 mm^2, 320 mm^3).

Figure 7 presents the number of terminal segments on each bifurcation level. It may be observed that just after the 4^{th} bifurcation some arteries are terminal. The number of terminal branches increases up to 9^{th} level where there are 19 terminal branches. The mean length of terminal arteries was 7.17 mm

Table 1. *Statistics of the main four sub–trees of the arterial system*

Sub–tree name	A	B	C	D
Number of branches and percent of total no. (total 178)	37 21%	78 44%	36 20%	27 15%
Convex hull circumscribed on the analyzed arterial sub–tree (mm3)	4284	24468	3067	2684
Radius of the artery in the root of the sub–tree (mm)	1.34	2.02	1.26	1.50
Area of the artery in the root of the sub–tree (mm2)	5.62	12.78	5.02	7.07
Volume of the arteries in the root of the sub–tree (mm3)	273.4	1002.1	217.01	226.65
Total length of the arteries in the sub–tree (mm)	212.8	527.78	171.96	152.94
Number of final segments in the sub–tree	16	39	17	1

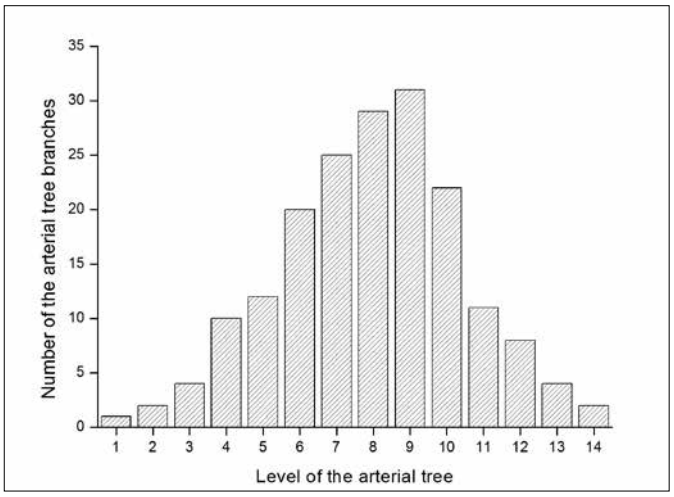

Figure 3. *Distribution of arterial branches (n = 181) at respective bifurcation levels.*

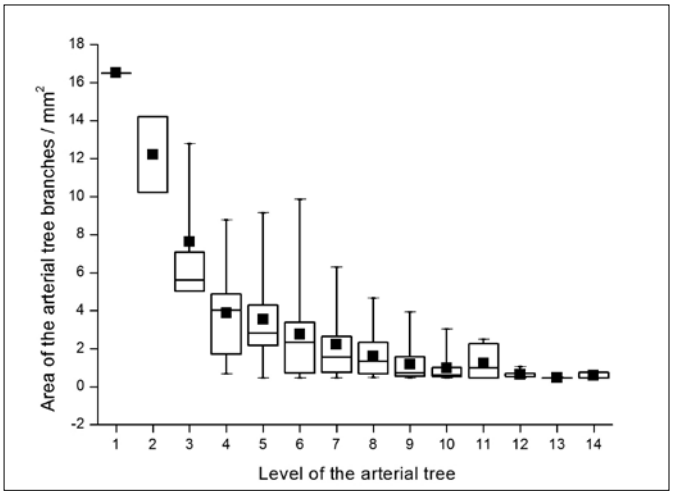

Figure 5. *Averaged segment area at respective bifurcation levels. The interpretation of graph symbols is identical to those used for Fig. 4.*

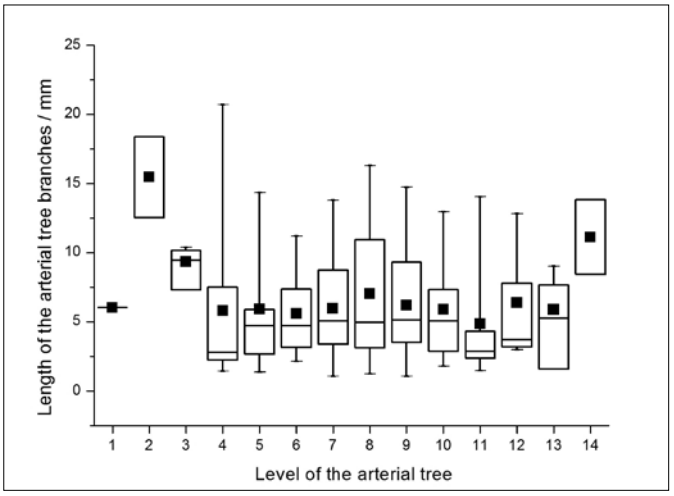

Figure 4. *Averaged segment length at respective bifurcation levels. Solid squares indicate the mean length of all vessel segments at a certain bifurcation level; vertical bars – minimum and maximum values; rectangles – lower and upper quartiles; horizontal line – median.*

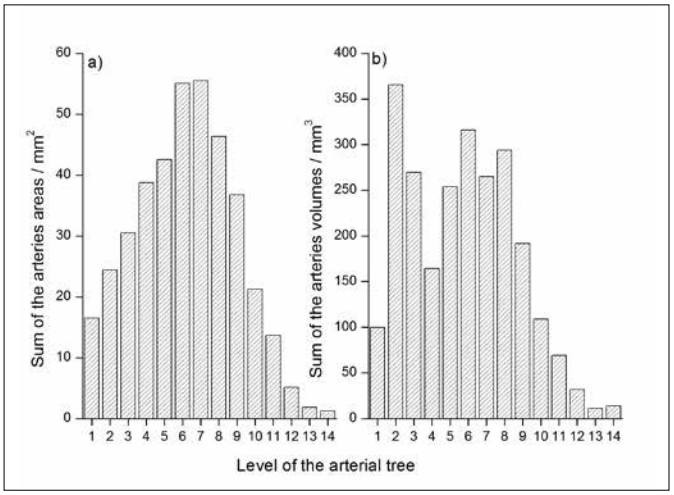

Figure 6. *Summary evaluation of the arteries at respective bifurcation levels: a) sum of the artery areas and b) sum of the artery volumes.*

(changing in the range from 1 mm to 15 mm) with standard deviation 3.67 mm. The mean radius was 0.46 mm (area was changing in the range from 0.5 \ to 1.5, only one 2.3 mm^2) with standard deviation 0.09 mm.

Also, a detailed analysis of the four main sub–trees (renal arterial segments) was done (Figure 1). Localization of the nodes in the renal space at the 6^{th} and 7^{th} bifurcation levels is presented in Figure 8. It may be noticed that arteries from different sub–trees occupy separate regions. For each sub–tree the following parameters were evaluated and relationships between them were observed. These were: number of branches, volume of convex hull circumscribed on each sub–tree, diameter and area of the artery in the sub–tree root, total length and volume of arteries and number of terminal segments. The calculated values of these parameters are presented in Table 1. In the presented endocast the total number of branches in four segments was 178. Each sub–tree consisted of 37 (21%), 78 (44%), 36 (20%), and 27 (15%) branches with volume of convex hull circumscribed on each segment of 4.28, 24.47, 3.07 and 2.68 cm^3, respectively.

We found a statistically significant correlation between all pairs of considered parameters. The value of the correlation coefficient in each case was greater than 0.89 and often was close to 0.99. It is very

important that the main sub–tree artery diameter is correlated with the number of branches (r = 0.89), volume of convex hull circumscribed on each sub–tree (r = 0.95), the total length (r = 0.93), the volume of the arteries in each sub–tree (r = 0.95), and the number of terminal segments (r = 0.91). Additionally, after conducting calculations and analyses with novel software tools, it may be concluded that the individual artery segments occupy a separate space in the kidney volume. A similar correlation is observed when the tree was divided into more sub–trees.

DISCUSSION

A serious complication of any intrarenal surgery is injury to major blood vessels. The anatomical relationship between the intrarenal arteries and kidney parenchyma was studied in XIX century with the beginning of kidney surgery. Analyzing kidney vessel endocasts, Hyrtl first discovered that the renal arterial system was divided into anterior and posterior part by the renal collecting system [19]. In 1901, Broedel described the branching of the renal artery in a tree–like pattern. In the same study, the avascular plane between the sub–tree of the renal artery was discovered [20]. In XX century, Graves, analyzing kidney endocasts, introduced a constant pattern of intrarenal artery arrangement, which divides the kidney cortex into specific anatomical segments [21]. The same anatomical segments are described in our study with the application of modern statistical tools. Our approach in this area is novel to our knowledge. The 3D statistical analyses provide data that can verify the previous descriptions of renal artery trees for practical implications during kidney surgery and can be applied in the preoperative planing.

CONCLUSIONS

Our observations confirmed that the kidney can be divided into segments with a separate arterial vascularization. The presented description of the methodology and the statistical analyses results, which enabled evaluation of the arterial system of the selected kidney, are a part of the project in which the greater set of objects will be tested. The verification of previous observations will contribute to our knowledge of the renal arterial system with in critical in precise Nephrong Sparing Surgery procedure.

ACKNOWLEDGEMENT

The authors would like to thank Maciej Augustyn MD, PhD for sharing kidney endocasts for further study.

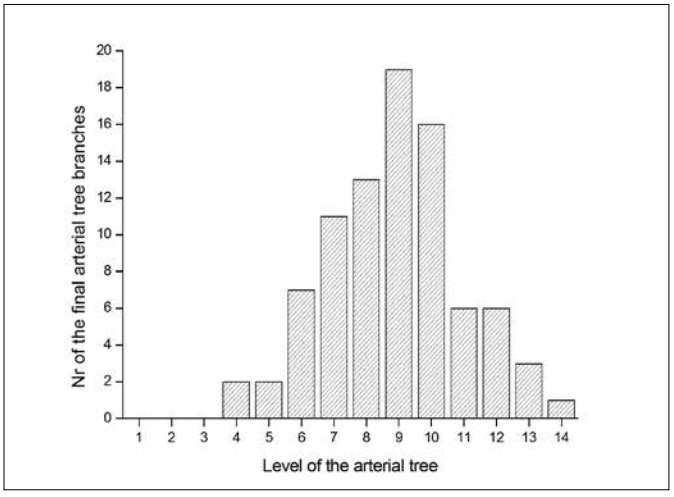

Figure 7. *Distribution of terminal segments (n = 86) at respective bifurcation levels.*

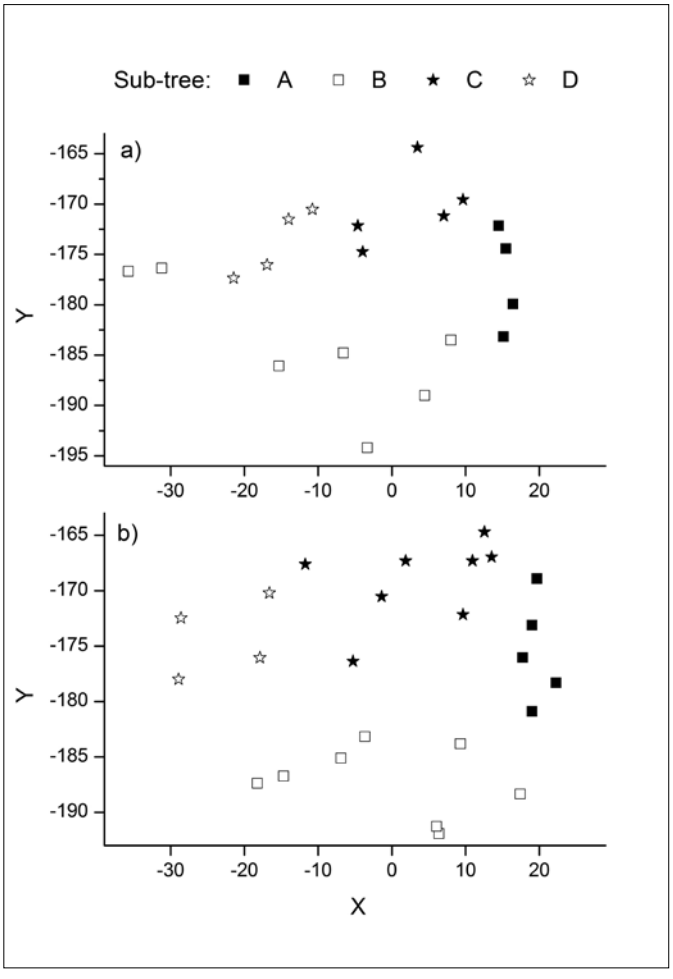

Figure 8. *Localization of the nodes (only X and Y coordinates from CT image) including bifurcation for the main four sub–trees: a) 6th level and b) 7th level. Denotation A, B, C, D corresponding to this in Table 1.*

References

1. Teber D, Baumhauer M, Guvenc EO, Rassweiler J. Robotic and imaging in urological surgery. Curr Opin Urol. 2009; 19: 108–113.

2. Pasticier G, Timsit M–O, Badet L, Abril L, Halila M, Fassi FH, et al. Nephron–sparing surgery for renal cell carcinoma: detailed analysis of complications over a 15–year period. Eur Urol. 2006; 49: 485–490.

3. Patard J–J, Pantuck AJ, Crepel M, Lam JS, Bellec L, Albouy B, et al. Morbidity and clinical outcome of nephron–sparing surgery in relation to tumour size and indication. Eur Urol. 2007; 52: 148–154.

4. Ljungberg B, Hanbury DC, Kuczyk MA. Renal cell carcinoma guidelines. Eur Urol. 2007; 51: 1502–1510.

5. Patard JJ, Shvarts O, Lam JS, Pantuck AJ, Kim HL, Ficarra V, Cindolo L, et al. Safety and efficacy of partial nephrectomy for all T1 tumours based on an international multicenter experience. J Urol. 2004; 171: 2181–2185.

6. Pahernik S, Roos F, Rohrig B, Wiesner C, Thuroff JWE. Elective nephron–sparing surgery for renal cell carcinoma larger than 4 cm. J Urol. 2008; 179: 71–74.

7. Leibovich BC, Blute ML, Cheville JC, Lohse CM, Weaver AL, Zincke H. Nephron–sparing surgery for appropriately selected renal cell carcinoma between 4 cm and 7 cm results in outcome similar to radical nephrectomy. J Urol. 2004; 171: 1066–1070.

8. Becker F, Siemer S, Hack M, Humke U, Ziegler M, Stockle M. Excellent long–term cancer control with elective nephron sparing surgery for selected renal cell carcinomas measuring more than 4 cm. Eur Urol. 2006; 49: 1058–1064.

9. Dash A, Vickers AJ, Schachter LR, Bach AM, Snyder ME, Russo P. Comparison of outcomes in elective partial versus radical nephrectomy for clear cell renal cell carcinoma of 4–7 cm. BJU Int. 2006; 97: 939–945.

10. Antonelli A, Cozzoli A, Nicolai M, Zani D, Zanotelli T, Perucchini L, et al. Nephron–sparing surgery versus radical nephrectomy in the treatment of intracapsular renal cell carcinoma up to 7 cm. Eur Urol. 2008; 53: 803–809.

11. Lin J, Knight EL, Hogan ML, Singh AK. A comparison of prediction equations for estimating glomerular filtration rate in adults without kidney disease. J Am Soc Nephrol. 2003; 14: 2573–2580.

12. Levey AS, Coresh J, Balk E, Kausz AT, Levin A, Steffes MW, et al. National Kidney Foundation practice guidelines for chronic kidney disease: evaluation, classification, and stratification. Ann Intern Med. 2003; 139: 137–147.

13. Huang WC, Levey AS, Serio AM, Snyder M, Vickers AJ, Raj GV, et al. Chronic kidney disease after nephrectomy in patients with renal cortical tumors: a retrospective cohort study. Lancet Oncol. 2006; 7: 735–740.

14. Family F, Masters BR, Platt DE. Fractal pattern formation in human retinal vessels. Physica. 1989; D38: 98–103.

15. Masters BR. Fractal analysis of normal human retinal blood vessels. Fractals. 1994; 2: 103–110.

16. Sonka M, Park W, Hoffman EA. Rule–based detection of intrathoracic airway trees. IEEE Transactions on Medical Imaging. 1996; 15: 314–326.

17. Bhuiyan E, Lamoureux B, Nath K, Ramamohanarao T, Wong Y. Retinal Image Matching Using Hierarchical Vascular Features. Comput Intell Neurosci. 2011 doi: 10.1155/2011/749054

18. Cormen TH, Leiserson CE, Rivest RL. Introduction to Algorithms. Cambridge: MIT Press, 2009.

19. Hyrtl J. Corrosions Anatomie. 1873; Vienna: Braunmuller, p. 240.

20. Broedl M. The intrinsic blood vessels of the kidney and their significance in nephrectomy. Bull. Johns Hopkins Hosp. 1901; 12: 10.

21. Graves FT. The anatomy of the intrarenal arteries and its application to segmental resection of the kidney. Br J Surg 1954; 42: 132–139.